EUROPEAN ORGANIZATION FOR NUCLEAR RESEARCH

CERN-PPE/91-121
July 31, 1991

An Investigation into Intermittency

The **ALEPH Collaboration**

Abstract

The results of an investigation based on ALEPH data, $e^+e^- \rightarrow$ hadrons at $\sqrt{s} = 91$ GeV, into fluctuations in rapidity space are presented. It is found that the behaviour of the factorial moments is well represented by the Lund parton shower model. An estimate is made of the scale of fluctuations needed to describe the data. Differential moments are introduced and are used to demonstrate that within the average represented by the traditional factorial moments the pattern of fluctuations is itself a strong function of rapidity. This pattern is shown to be primarily associated with the emission of hard gluons. The implied structure between the hadron clusters and partons is explored by the use of transverse mass moments. It is concluded that the principal features of the one-dimensional factorial moments, differential moments and transverse mass moments have their origin in the $O(\alpha_s)$ matrix element, kinematic boundaries and the method of selection of the event axis.

Submitted to Zeitschrift für Physik C

The ALEPH Collaboration

D. Decamp, B. Deschizeaux, C. Goy, J.-P. Lees, M.-N. Minard

Laboratoire de Physique des Particules (LAPP), IN²P³-CNRS, 74019 Annecy-le-Vieux Cedex, France

R. Alemany, J.M. Crespo, M. Delfino, E. Fernandez, V. Gaitan, Ll. Garrido, Ll.M. Mir, A. Pacheco

Laboratorio de Fisica de Altas Energias, Universidad Autonoma de Barcelona, 08193 Bellaterra (Barcelona), Spain[8]

M.G. Catanesi, D. Creanza, M. de Palma, A. Farilla, G. Iaselli, G. Maggi, M. Maggi, S. Natali, S. Nuzzo, M. Quattromini, A. Ranieri, G. Raso, F. Romano, F. Ruggieri, G. Selvaggi, L. Silvestris, P. Tempesta, G. Zito

INFN Sezione di Bari e Dipartimento di Fisica dell' Università, 70126 Bari, Italy

Y. Gao, H. Hu,[21] D. Huang, X. Huang, J. Lin, J. Lou, C. Qiao,[21] T. Ruan,[21] T. Wang, Y. Xie, D. Xu, R. Xu, J. Zhang, W. Zhao

Institute of High-Energy Physics, Academia Sinica, Beijing, The People's Republic of China[9]

W.B. Atwood,[2] L.A.T. Bauerdick, F. Bird,[4] E. Blucher, G. Bonvicini, F. Bossi, J. Boudreau, D. Brown, T.H. Burnett,[3] H. Drevermann, R.W. Forty, C. Grab,[23] R. Hagelberg, S. Haywood, J. Hilgart, B. Jost, M. Kasemann,[28] J. Knobloch, A. Lacourt, E. Lançon, I. Lehraus, T. Lohse, A. Lusiani, A. Marchioro, M. Martinez, P. Mato, S. Menary, A. Minten, A. Miotto, R. Miquel, H.-G. Moser, J. Nash, P. Palazzi, F. Ranjard, G. Redlinger, A. Roth, J. Rothberg,[3] H. Rotscheidt, M. Saich, D. Schlatter, M. Schmelling, M. Takashima, W. Tejessy, H. Wachsmuth, S. Wasserbaech, W. Wiedenmann, W. Witzeling, J. Wotschack

European Laboratory for Particle Physics (CERN), 1211 Geneva 23, Switzerland

Z. Ajaltouni, F. Badaud, M. Bardadin-Otwinowska, A.M. Bencheikh, R. El Fellous, A. Falvard, P. Gay, C. Guicheney, J. Harvey, P. Henrard, J. Jousset, B. Michel, J-C. Montret, D. Pallin, P. Perret, J. Proriol, F. Prulhière, G. Stimpfl

Laboratoire de Physique Corpusculaire, Université Blaise Pascal, IN²P³-CNRS, Clermont-Ferrand, 63177 Aubière, France

J.D. Hansen, J.R. Hansen, P.H. Hansen, R. Møllerud, B.S. Nilsson

Niels Bohr Institute, 2100 Copenhagen, Denmark[10]

I. Efthymiopoulos, E. Simopoulou, A. Vayaki

Nuclear Research Center Demokritos (NRCD), Athens, Greece

J. Badier, A. Blondel, G. Bonneaud, J. Bourotte, F. Braems, J.C. Brient, G. Fouque, A. Gamess, R. Guirlet, S. Orteu, A. Rosowsky, A. Rougé, M. Rumpf, R. Tanaka, H. Videau

Laboratoire de Physique Nucléaire et des Hautes Energies, Ecole Polytechnique, IN²P³-CNRS, 91128 Palaiseau Cedex, France

D.J. Candlin, E. Veitch

Department of Physics, University of Edinburgh, Edinburgh EH9 3JZ, United Kingdom[11]

L. Moneta, G. Parrini

Dipartimento di Fisica, Università di Firenze, INFN Sezione di Firenze, 50125 Firenze, Italy

M. Corden, C. Georgiopoulos, M. Ikeda, J. Lannutti, D. Levinthal,[16] M. Mermikides, L. Sawyer

Supercomputer Computations Research Institute and Dept. of Physics, Florida State University, Tallahassee, FL 32306, USA [13,14,15]

A. Antonelli, R. Baldini, G. Bencivenni, G. Bologna,[5] P. Campana, G. Capon, F. Cerutti, V. Chiarella, B. D'Ettorre-Piazzoli,[6] G. Felici, P. Laurelli, G. Mannocchi,[6] F. Murtas, G.P. Murtas, G. Nicoletti, L. Passalacqua, M. Pepe-Altarelli, P. Picchi,[5] P. Zografou

Laboratori Nazionali dell'INFN (LNF-INFN), 00044 Frascati, Italy

B. Altoon, O. Boyle, A.W. Halley, I. ten Have, J.L. Hearns, J.G. Lynch, W.T. Morton, C. Raine, J.M. Scarr, K. Smith, A.S. Thompson, R.M. Turnbull

Department of Physics and Astronomy, University of Glasgow, Glasgow G12 8QQ, United Kingdom[11]

B. Brandl, O. Braun, R. Geiges, C. Geweniger, P. Hanke, V. Hepp, E.E. Kluge, Y. Maumary, A. Putzer, B. Rensch, A. Stahl, K. Tittel, M. Wunsch

Institut für Hochenergiephysik, Universität Heidelberg, 6900 Heidelberg, Fed. Rep. of Germany[17]

A.T. Belk, R. Beuselinck, D.M. Binnie, W. Cameron, M. Cattaneo, P.J. Dornan,[1] S. Dugeay, A.M. Greene, J.F. Hassard, N.M. Lieske, S.J. Patton, D.G. Payne, M.J. Phillips, J.K. Sedgbeer, G. Taylor, I.R. Tomalin, A.G. Wright

Department of Physics, Imperial College, London SW7 2BZ, United Kingdom[11]

P. Girtler, D. Kuhn, G. Rudolph

Institut für Experimentalphysik, Universität Innsbruck, 6020 Innsbruck, Austria[19]

C.K. Bowdery,[1] T.J. Brodbeck, A.J. Finch, F. Foster, G. Hughes, N.R. Keemer, M. Nuttall, A. Patel, B.S. Rowlingson, T. Sloan, S.W. Snow, E.P. Whelan

Department of Physics, University of Lancaster, Lancaster LA1 4YB, United Kingdom[11]

T. Barczewski, K. Kleinknecht, J. Raab, B. Renk, S. Roehn, H.-G. Sander, H. Schmidt, F. Steeg, S.M. Walther, B. Wolf

Institut für Physik, Universität Mainz, 6500 Mainz, Fed. Rep. of Germany[17]

J-P. Albanese, J-J. Aubert, C. Benchouk, V. Bernard, A. Bonissent, D. Courvoisier, F. Etienne, S. Papalexiou, P. Payre, B. Pietrzyk, Z. Qian, M. Talby,[1]

Centre de Physique des Particules, Faculté des Sciences de Luminy, IN²P³-CNRS, 13288 Marseille, France

H. Becker, W. Blum, P. Cattaneo, G. Cowan, B. Dehning, H. Dietl, F. Dydak[26], M. Fernandez-Bosman, T. Hansl-Kozanecka,[2,22] A. Jahn, W. Kozanecki,[2] E. Lange, J. Lauber, G. Lütjens, G. Lutz, W. Männer, Y. Pan, R. Richter, J. Schröder, A.S. Schwarz, R. Settles, U. Stierlin, R. St. Denis, J. Thomas, G. Wolf

Max-Planck-Institut für Physik und Astrophysik, Werner-Heisenberg-Institut für Physik, 8000 München, Fed. Rep. of Germany[17]

V. Bertin, J. Boucrot, O. Callot, X. Chen, A. Cordier, M. Davier, G. Ganis, J.-F. Grivaz, Ph. Heusse, P. Janot, D.W. Kim,[20] F. Le Diberder, J. Lefrançois,[1] A.-M. Lutz, J.-J. Veillet, I. Videau, Z. Zhang, F. Zomer

Laboratoire de l'Accélérateur Linéaire, Université de Paris-Sud, IN²P³-CNRS, 91405 Orsay Cedex, France

D. Abbaneo, S.R. Amendolia, G. Bagliesi, G. Batignani, L. Bosisio, U. Bottigli, C. Bradaschia, M. Carpinelli, M.A. Ciocci, R. Dell'Orso, I. Ferrante, F. Fidecaro, L. Foà, E. Focardi, F. Forti, C. Gatto, A. Giassi, M.A. Giorgi, F. Ligabue, E.B. Mannelli, P.S. Marrocchesi, A. Messineo, L. Moneta, F. Palla, G. Sanguinetti, J. Steinberger, R. Tenchini, G. Tonelli, G. Triggiani, C. Vannini, A. Venturi, P.G. Verdini, J. Walsh

Dipartimento di Fisica dell'Università, INFN Sezione di Pisa, e Scuola Normale Superiore, 56010 Pisa, Italy

J.M. Carter, M.G. Green,[1] P.V. March, T. Medcalf, I.S. Quazi, J.A. Strong, R.M. Thomas, L.R. West, T. Wildish

Department of Physics, Royal Holloway & Bedford New College, University of London, Surrey TW20 OEX, United Kingdom[11]

D.R. Botterill, R.W. Clifft, T.R. Edgecock, M. Edwards, S.M. Fisher, T.J. Jones, P.R. Norton, D.P. Salmon, J.C. Thompson

Particle Physics Dept., Rutherford Appleton Laboratory, Chilton, Didcot, Oxon OX11 OQX, United Kingdom[11]

B. Bloch-Devaux, P. Colas, C. Klopfenstein, E. Locci, S. Loucatos, E. Monnier, P. Perez, J.A. Perlas, F. Perrier, J. Rander, J.-F. Renardy, A. Roussarie, J.-P. Schuller, J. Schwindling, B. Vallage

Département de Physique des Particules Elémentaires, CEN-Saclay, 91191 Gif-sur-Yvette Cedex, France[18]

J.G. Ashman, C.N. Booth, C. Buttar, R. Carney, S. Cartwright, F. Combley, M. Dinsdale, M. Dogru, F. Hatfield, J. Martin, D. Parker, P. Reeves, L.F. Thompson

Department of Physics, University of Sheffield, Sheffield S3 7RH, United Kingdom[11]

E. Barberio, S. Brandt, H. Burkhardt,[1] C. Grupen, H. Meinhard, L. Mirabito, U. Schäfer, H. Seywerd

Fachbereich Physik, Universität Siegen, 5900 Siegen, Fed. Rep. of Germany[17]

G. Giannini, B. Gobbo, F. Ragusa,[25] L. Rolandi, U. Stiegler

Dipartimento di Fisica, Università di Trieste e INFN Sezione di Trieste, 34127 Trieste, Italy

L. Bellantoni, X. Chen, D. Cinabro, J.S. Conway, D.F. Cowen,[24] Z. Feng, D.P.S. Ferguson, Y.S. Gao, J. Grahl, J.L. Harton, J.E. Jacobsen, R.C. Jared,[7] R.P. Johnson, B.W. LeClaire, Y.B. Pan, J.R. Pater, Y. Saadi, V. Sharma, Z.H. Shi, Y.H. Tang, A.M. Walsh, J.A. Wear,[27] F.V. Weber, M.H. Whitney, Sau Lan Wu, G. Zobernig

Department of Physics, University of Wisconsin, Madison, WI 53706, USA[12]

(Submitted to Zeitschrift für Physik C)

---

[1] Now at CERN.
[2] Permanent adddress: SLAC, Stanford, CA 94309, USA.
[3] Permanent address: University of Washington, Seattle, WA 98195, USA.
[4] Now at SSCL, Dallas, TX, U.S.A.
[5] Also Istituto di Fisica Generale, Università di Torino, Torino, Italy.
[6] Also Istituto di Cosmo-Geofisica del C.N.R., Torino, Italy.
[7] Permanent address: LBL, Berkeley, CA 94720, USA.
[8] Supported by CAICYT, Spain.
[9] Supported by the National Science Foundation of China.
[10] Supported by the Danish Natural Science Research Council.
[11] Supported by the UK Science and Engineering Research Council.
[12] Supported by the US Department of Energy, contract DE-AC02-76ER00881.
[13] Supported by the US Department of Energy, contract DE-FG05-87ER40319.
[14] Supported by the NSF, contract PHY-8451274.
[15] Supported by the US Department of Energy, contract DE-FC0S-85ER250000.
[16] Supported by SLOAN fellowship, contract BR 2703.
[17] Supported by the Bundesministerium für Forschung und Technologie, Fed. Rep. of Germany.
[18] Supported by the Institut de Recherche Fondamentale du C.E.A.
[19] Supported by Fonds zur Förderung der wissenschaftlichen Forschung, Austria.
[20] Supported by the Korean Science and Engineering Foundation and Ministry of Education.
[21] Supported by the World Laboratory.
[22] On leave of absence from MIT, Cambridge, MA 02139, USA.
[23] Now at ETH, Zürich, Switzerland.
[24] Now at California Institute of Technology, Pasadena, CA 91125, USA.
[25] Now at Dipartimento di Fisica, Università di Milano, Milano, Italy.
[26] Also at CERN, PPE Division, 1211 Geneva 23, Switzerland.
[27] Now at University of California, Santa Cruz, CA 95064, USA.
[28] Now at DESY, Hamburg, Germany.

1 Introduction and Overview

Intermittency is a term derived from turbulence theory to describe one of the routes which a system takes in going from a stable to a chaotic state. This transition is displayed by characteristic observables of the system having randomly occurring spikes in the distributions of appropriate variables. In high energy physics the spikes could correspond to particle clusters. Many physical effects could lead to such clustering. The analysis of moments of particle distributions in high energy physics was proposed by Bialas and Peschanski [1], originally in connection with identifying a quark-gluon plasma. In most analyses the moments have been applied to rapidity distributions of the tracks to give information on particle correlations in rapidity space. The subject of this paper is their application to ALEPH data on $e^+e^- \rightarrow$ hadrons at the Z peak where large effects are observed.

There are two main approaches to the interpretation of intermittency. In the first approach the phenomenon is discussed in terms of the magnitude and form of clustering as a function of scale. One concern is the extent to which the data may show self similarity at different scales, possibly reflecting some internal cascade processes. Such an analysis is often presented in terms of a scale-dependent fractal dimension. The second approach uses the fact that some models of hadronisation, such as the Lund parton shower (PS) Monte Carlo [2], describe the intermittency effect seen in the data. The Monte Carlo models are studied and used to understand the underlying physics creating the effect. This investigation adopts the second approach and focuses on the question 'Why do the one dimensional moments in rapidity space behave as they do?'

Ochs [3] has argued for a general analysis in terms of the scaling properties of multiplicity functions and their relationship with behaviour at the parton level. Sjöstrand has stated that parton-induced jets are important in rapidity correlations [4], and that an intermittency signal from jets does *not* have to be related to a parton cascade mechanism; even 3-jet events alone should show the effect. By contrast, Gustafson and Sjogren [5], and Gustafson [6], have emphasized the importance of the parton cascade in explaining the observed behaviour of the moments, but they also noted the importance of directly produced pions from string fragmentation. However, there have been uncertainties in the significance of different processes and their relative contribution to the creation of an intermittency signal. It is clear that perturbative effects should be of increased importance at LEP energies compared with data from PEP and PETRA, as OPAL [7] indicates.

Event selection and simulation are described in section 2. In section 3, hadron correlations in ALEPH data are analysed in rapidity space using a factorial moment analysis. These moments are referred to here as 'global moments' to indicate that the whole range of y considered is included in the moment calculation. The results are in agreement with the conclusion from DELPHI [8] and OPAL that the behaviour of the

moments at LEP energies is well described by the parton shower model. In section 4, differential moments are introduced and are shown to be strong functions of rapidity. The shape and magnitude of these functions are also well described by the Lund PS model. It is found that the dependence on rapidity is greatly reduced if the perturbative QCD effects are not included in the simulation. In section 5, a weighting procedure is introduced to investigate this by replacing the number of hadrons in a rapidity bin by a boost-invariant measure, their transverse mass. A direct comparison is made between transverse mass moments for data and Monte Carlo at the hadron level, and then between hadrons and partons using the Monte Carlo. It is shown in section 6 that the essential features of the one dimensional differential and transverse mass moments have their origin in the $O(\alpha_s)$ matrix element, kinematic boundaries and the use of the thrust axis for rapidity determination. Summary and conclusions are given in section 7.

2 Event Selection and Simulation

The ALEPH detector is described in detail elsewhere [9]. Charged tracks are measured over the range $|\cos(\theta)| < 0.95$, where θ is the polar angle, by an inner cylindrical drift chamber, the ITC, and a time projection chamber, the TPC. These together with a solenoidal field of 1.5 Tesla give a momentum resolution of $\delta p/p^2 = 0.0008\ (GeV/c)^{-1}$.

The analysis is based on a sample of ALEPH 1990 data on e^+e^- at energies close to the Z resonance peak. Trigger inefficiency was negligible. Acceptable tracks were required to have at least four coordinates measured by the TPC, a polar angle with respect to the beam axis in the range 20° to 160°, a transverse momentum, P_t, with respect to the beam axis $\geq$ 200 MeV/c, and to extrapolate to within 2 cm (d_o) of the beam axis, and 5 cm (z_o) of the interaction point. Selected events were required to have at least 5 such tracks in the appropriate rapidity range; after cuts, approximately 80K events were analysed. The thrust axis was found from the accepted tracks, and was required to have a polar angle $35° < \theta < 145°$.

The Lund PS model gives a very good general description of hadron events and of intermittency effects, as shown later. For direct comparison with data, Monte Carlo events (approximately 70K) with complete detector and experimental event selection were generated using as input JETSET 6.3 specially tuned [10] to match the data on inclusive and event shape variables. These are referred to as GALEPH [GEANT + ALEPH] events after the name of the simulation program. The investigations were based on generator level Monte Carlo events created with the same parameter values. All particles with a mean lifetime of less than 1 ns were required to decay, the others were treated as stable. The effects of the detector and experimental cuts were checked by comparing the results of the two Monte Carlo sets for the variables studied, and were found not to affect the physics conlusions. Appropriate variations in the parameters

could then be introduced at the generator level and comparisons made between the hadron and the parton level without the need for correction for detector effects. The aim of this paper is to find a physics explanation and so no corrections are applied to the data here.

3 Global Factorial Moments

3.1 Method

The rapidities with respect to the thrust axis of all charged particles in a hadronic event are calculated assuming the pion mass using the formula

$$y = 0.5 \ln[(E + p_{||})/(E - p_{||})] \tag{1}$$

where E is the energy and $p_{||}$ the momentum component of the hadron along this axis. The interval Δy, $-2 \leq y \leq 2$, is divided into M equal bins of width $\Delta y/M$. From the number, n_m, of particles in the m^{th} bin, the quantities

$$(S_i)_m = n_m(n_m - 1)\ldots(n_m - i + 1) \tag{2}$$

are found for each bin.

Two slightly different definitions of the factorial moments are commonly used, referred to here as standard moments and normalized moments $F_i^s(M)$ and $F_i^n(M)$ respectively.

$$F_i^s(M) := \frac{\langle \frac{1}{M} \sum_{m=1}^{M} (S_i)_m \rangle \; M^i}{\langle N \rangle^i} \tag{3}$$

$$F_i^n(M) := \langle \frac{\frac{1}{M} \sum_{m=1}^{M} (S_i)_m \; M^i}{N(N-1)\ldots(N-i+1)} \rangle \tag{4}$$

N is the total number of particles in the Δy range, typically 12. Both moments are sensitive to any local correlations in particle number density within the range Δy. Both expressions average to unity for a random distribution, in which both the total number of particles and the number in each bin have Poisson distributions. The normalisation of the standard moments includes the mean multiplicity of events, and so they are sensitive to the shape of the distribution in N, whereas this dependency is removed in the normalized moments. The higher moments give greater weight to larger clusters of tracks in the bins and to some extent contain information held in the lower moments.

3.2 Results

Figures 1a,b show that the Lund PS model agrees well with the data for the standard and normalized moments. Changes in the cuts, in d_o from 0.5 to 3 cm, in z_o from 3 to 6 cm, in the minimum polar angle of a track with respect to the beam axis from 15 to 25 degrees, and in the cosine of the polar angle of the thrust axis from 0.5 - 0.8, had little effect on the data. Only the P_t cut was found to make a significant change in the analysis and will be discussed later.

The results show, as do those of DELPHI and OPAL, that the Lund PS model is in quantitative agreement with data at LEP energies. CELLO [11] made a general 3-dimensional analysis using cells in Lorentz invariant phase space, from which they concluded that no new physics was required to describe the data. TASSO [12] analysis gave no conclusive evidence as to the agreement of the models, but it was shown there that 2-jet events displayed a weaker intermittency signal; TASSO also introduced the normalized moments. The general conclusion is that the use of the Lund model could lead to the understanding of which effects are important in contributing to the signal detected.

3.3 A Simple Model

To give an indication of the magnitude of the effects needed to account for such moments, comparison is made with a simple model of a fluctuation process in which, within a constant $\langle dN/dy \rangle$ there are two contributions to the hadrons, each of which is Poissonian. One process contributes uniformly over the full y range of interest with a total number of particles n_1. The second component extends over a fraction f of the full y range, within which it raises the mean level by a factor β. The position of this component is to be randomly distributed over the full y range. One could picture some physics process which superimposes a local clustering of particles and which itself could occur anywhere within the y range, on top of the main, structureless background. The model assumes that every event is of this nature.

Taking $\langle N \rangle = 12$ to match the data over the interval $|y| \leq 2$, there are effectively just two parameters of the model, f and β. The fraction, f, controls the value of M at which the moments start to saturate with increasing M, roughly at $M = 1/f$. The parameter β controls the asymptotic values of the moments at high M, though not their relative magnitudes. For a Poisson distribution both the standard and the normalized moments equal 1.0 for $M = 1$, whereas the moments are higher in the data, reflecting a non- Poissonian distribution. No attempt is made to simulate a non-Poisson distribution in total N, and therefore comparison of the simple model is made to the normalized moments. With appropriate choices of β and f, quite a reasonable description of the

data is possible. This is shown in figure 2 with $\beta = 3.5$ and $f = 0.35$. The agreement, including the relative magnitudes, is surprisingly good in view of the simplicity of the assumptions.

The parameters of the simple model indicate the magnitude of the effects needed to account for the observed behaviour of the moments, namely, that there has to be some process that can increase the density of the tracks over about 1.4 units of rapidity space by an average factor of about 3.5 – not necessarily constant of course, as the process itself could be subject to fluctuations. This magnitude would have to be even greater if only a fraction of the events were affected.

The model can also serve to demonstrate some of the more general features of moments analysis. Moments increase with M because as long as the fluctuations occur within a single bin, $\Delta y/M$, the narrower this bin the greater their significance. In the limit in which the mean number of particles, $n_1.f(\beta - 1)$, in the fluctuation is held constant while the width f tends to zero, the moments will exhibit a power law rise $F_i^n(M)$ proportional to M^{i-1} in the range $1 \ll M \ll f^{-1}$. This is a simple example of scale invariance leading to a power law dependence. It should be mentioned that this simple model is not expected to be successful in higher dimensions.

4 Differential Moments

4.1 Method

The moments which have been used so far do not contain information on the distribution in y of the fluctuations, because they are averaged over the entire range. It is useful to know if the moments are uniform with y, or if they tend to cluster in particular regions as can occur, for example, for b quark decays in data also containing light quarks. The differential moments are introduced in order to study the y dependence of the fluctuations and are calculated as follows: the value, $(S_i)_m$ (equation 2), is given for each of the M individual bins across the y range. The average over all events,

$$(f_i)_m = \langle (S_i)_m \rangle / \langle n_m \rangle^i \tag{5}$$

is taken. The denominator, the mean number of tracks in the bin, ensures that for a Poisson distribution $f_i = 1.0$ for all i. Since each y bin is analysed with respect to its own mean, there is no longer any need for a relatively flat y distribution, and the differential moments can be used to study the fluctuations in regions where the rapidity density is varying rapidly. Therefore, a range $-4 \leq y \leq 4$ is used, which includes the majority of particles produced. As all the global moments showed similar

behaviour, attention is focused on the third moment, f_3, in order to limit the number of combinations; the statistical errors are small and any effect of gamma conversions is reduced due to the weighting of the third moment. The average value of a moment at a given y will be unchanged under changes in M, or bin width, if the particles within that bin are uncorrelated. This is important in following the evolution of the structure as a function of M.

4.2 Results and Interpretation

Figures 3 show the rapidity distributions for the data and Monte Carlo. It can be seen that data and the GALEPH Monte Carlo agree very well. At generator level the most significant effect is a much reduced central dip. Figure 3d demonstrates that this effect is mainly due to the P_t cut of 200 MeV/c on tracks. The global moments average over such variations.

The differential moment f_3 is shown in figure 4 over an extended range of y. Beyond $|y| = 2.0$, where the density is falling very rapidly with increasing $|y|$, f_3 is almost constant with a value of about 1.5 which is close to the Poissonian value of 1. Main attention is directed to the central region of $|y| < 2.0$, where two peaks apper near $|y| = 0.6$. The horizontal line shows the corresponding global moment $F_3'(M = 16)$. It is seen that within this average there is a rapid and striking variation in the pattern of fluctuations as measured by f_3. The differential moments are independent of the averge rapidity density in a bin because they are normalized by it. The peaks in the differential moments are narrower than, and displaced from, those in particle density.

Figure 5 shows the evolution of the differential moment, f_3, with increasing M. This corresponds to the evolution seen in the rise of the global moments (figure 1a). The central structure changes, with the peak increasing from 6.5 to 8.0 when M is doubled from 16 to 32. The values at high $|y|$ scarcely change. These results are also insensitive to the variations in the cuts on tracks and events described in section 3.2.

Figure 6 shows the difference in the moments according to whether the event axis was chosen to be thrust or sphericity for the calculation of rapidity. It can be seen that in the central region, $|y| < 1$, the dip structure disappears if sphericity is used. The explanation is given in section 6.

Investigations were carried out using the Monte Carlo to determine the source of the correlations. At generator level the magnitudes of the moments are decreased, relative to those with experimental detector and cut simulation, within the region $|y| < 1$, as seen in figure 7, but the structure has the same general shape thus retaining the same physics. The rest of the section deals with these analyses.

The effect of variations in particle density as a function of flavour was small; Monte Carlo studies show that this is greatest around $|y| = 2$ for $\bar{b}b$ events, which are only 1/5 of the total. In the moments, light and heavy quarks investigated alone showed the same general structure. It was also verified that the assignment of the pion mass to all charged tracks had a negligible effect on the moments.

A high particle multiplicity on one side of an event in rapidity is often associated with high gluon energy flow on the same side. This relationship was most directly tested by switching off the perturbative QCD effects, equivalent, in string model language, to removing the kinks in the string. The effect on the moments can be seen in figure 8a. There is still a significant though much smaller structure at $|y| = 2.6$. This is principally the effect of the admixture of $\bar{b}b$ in the simulation which produces a high particle multiplicity in this region when there is a hard fragmentation function and no gluon radiation.

The total mean number of charged particles in this last test fell from about 20 to 12. The significance of clustering must be compared with that expected from Poisson statistics for a given mean; to correct for this, the Lund fragmentation parameter, a, was increased from 0.5 to 4.0 (with all other parameters unchanged), giving a mean of 20. Figure 8b gives the result. Effects such as decays, flavour admixture, and hadronisation are present in similar proportions in the non-perturbative and Lund PS distributions. The differential moments decrease, because residual fluctuations become relatively smaller with respect to the increased means. The absolute values are also closer to Poissonian. Jet-like structures produced by perturbative QCD are the most important effect.

These results should not be taken to exclude contributions to intermittency from non-perturbative processes in general, for example the CELLO [11] analysis. The reference to a rapidity axis emphasizes particular kinds of fluctuation, such as those from jets, and the restriction to one dimension can, as emphasized by Ochs [3], average over and thereby weaken other contributions. The investigation indicates that the main behaviour of the global and differential moments in rapidity has its origin at the parton level and that their study can be a simple way of examining parton-induced effects in the event sample. The nature of these effects is such that any of the higher moments could also have been chosen for the study, as shown by figure 1a. The exploration of the relationship between partons and hadrons as it affects intermittency is described in the next two sections.

5 Transverse Mass

5.1 Definition

The previous investigation has dealt solely with fluctuations in hadron number density, this being the main tool of intermittency analysis. However, hadrons with a given rapidity cover a wide spectrum of energies particularly in the important central region where rapidity becomes essentially a function of polar angle alone. It is proposed here that the source of the fluctuations comes from the superposition of events with a gluon contribution to the y distribution, and therefore the significance of a fluctuation should lie also in the associated energies, rather than merely the number, of hadrons in a rapidity bin. In order to pursue this idea the simplest procedure would be to weight each hadron in a given rapidity bin by its energy, effectively replacing hadron number by total hadron energy. This however introduces a major disadvantage in studying y dependence because energy density is not invariant under boosts along the rapidity axis as is the number density. This problem is avoided by the following procedure. Hadrons are allocated to bins in y as before and the quantity:

$$M_t = \sqrt{\sum(E + P_{||}) \sum(E - P_{||})} \tag{6}$$

for the set of tracks in each bin is calculated. This quantity is referred to as the transverse mass of the set of hadrons and reduces to the total energy at $y = 0$; it is invariant under boosts in y. It can be applied at both the hadron and the parton level. Its use will also lead to an explanation at the parton level of why the differential moments have the observed structure in y, and why the choice of thrust rather than sphericity is important in the determination of the rapidity axis.

5.2 Results

It is convenient to examine the y dependence in terms of one of the higher moments of the transverse mass distribution. Such a moment gives a single number at each y value and emphasizes the high mass tail of the distribution, as did the higher factorial moments emphasize the high multiplicity tail in the hadron multiplicity distributions. Attention is again directed to the third moment, $\langle {M_t}^3 \rangle$ which is shown for data and Monte Carlo as a function of y in figure 9. The general structure is even clearer in the transverse mass moments where the fall at high y seen in the differential moments is accentuated. The Monte Carlo can now be used to make a direct comparison between hadrons and partons at generator level. The gluon mass is taken as zero and the default Lund values are used for the quarks. The moments for the hadrons are shown in figure 10a and for the partons in 10b. The similarity in the shape of the transverse mass

moments is confirmation that the structure seen in the various moments at hadron level has its origin at the parton level. Monte Carlo studies have shown that the major source of the relative magnitude of difference between the hadrons and partons is mainly due to missing transverse mass resulting from the use of charged hadrons only. If, as before, the perturbative processes are switched off, the moments become very small (figure 10a,b). The discontinuities in the moments in figure 10b, just below $|y| = 3.0$, are produced by b quark events, which have a maximum rapidity at this value because of the large b quark mass.

6 The Origin of the Structure

It has been shown with the differential moments and confirmed with the transverse mass moments that the origin of the intermittency effect is at the parton level. The purpose of this section is to relate the basic parton level physics to what is being seen in the data.

To $O(\alpha_s)$, the cross section for the process $e^+e^- \longrightarrow \bar{q}qg$ is given in terms of fractional energies x_i by

$$\frac{d\sigma}{\sigma} = \frac{2\alpha_s}{3\pi} \frac{({x_1}^2 + {x_3}^2)}{(1-x_1)(1-x_3)} dx_1 dx_3 \tag{7}$$

where $x_1 = E_{quark}/E_{beam}$ refers to the quark, x_2 to the gluon and x_3 to the antiquark, all assumed massless. The axis is taken along and in the direction of the quark. The scaled transverse mass, $m_t = M_t/E_{beam} = x_2 \sin\theta_{21} = x_3 \sin\theta_{31}$, where θ_{ij} is the angle between partons i and j; the transverse mass of individual, massless partons is the same as the transverse momentum. The quark and gluon together have a large transverse mass but zero transverse momentum. For the gluon $y = \ln(\cot\theta_{21}/2)$, and for the antiquark: $y = \ln(\cot\theta_{31}/2)$. Transforming to the $m_t - y$ plane, the cross-section for the emission of a gluon becomes:

$$\frac{d\sigma}{\sigma} = \frac{4\alpha_s}{3\pi} ({x_1}^2 + {x_3}^2) \frac{dm_t dy}{m_t} \tag{8}$$

Apart from the slowly varying quadratic factor, the density on the $m_t - y$ plane falls as $1/m_t$ and is independent of y. For any given y there is a kinematic limit on the maximum value of M_t which, along with the density distribution, controls the value of the moment. The result is a smooth, structureless variation in the moments with

y. The central structure seen in the moments has some origin other than the matrix element probability.

The density in the $m_t - y$ plane above was calculated with respect to the quark direction, while in the analysis the axis is chosen to maximise the event thrust. The corresponding procedure at the parton level causes the axis to align near to the most energetic parton. If the variables are re-evaluated with respect to the thrust axis then the distributions in the $m_t - y$ plane split such that the central dip emerges in m_t as a function of y. The predicted positions of the peaks, namely $|y| = \ln(\tan 60°) = 0.55$, correspond closely with those seen in the differential moments.

The difference in the moments defined with respect to the thrust or sphericity axis can also be seen at the parton level. In an event with two equally energetic partons and a third smaller energy parton (an example of the type of event which populates the central region of the rapidity distribution), the sphericity axis will be along the symmetry axis of the event. The thrust will choose one or the other of the two high energy partons creating the kinematic splitting described above. No corresponding choice occurs with sphericity and therefore no dip structure is produced.

7 Summary and Conclusions

The global moments, standard and normalized, have been presented for charged particles in rapidity space for ALEPH data. Rapidity was measured with respect to the thrust axis. Lund PS reproduced the data well, in agreement with the DELPHI and OPAL results.

The magnitude of the fluctuations in particle density required to match those observed in the data was estimated by comparison with a simple model, and found to correspond to local increases in the density of tracks of a factor 3.5 over a range of 1 - 1.5 units of y. The introduction of differential moments showed that the fluctuations themselves have a strong y dependence, with sharp peaks near $|y| = 0.6$. These moments give detailed information on the fluctuations over the rapidity range. The only source of fluctuations of the required magnitude, found on the considered scale, arose from perturbative QCD effects. When the gluon radiation was switched off, corresponding to the fragmentation of a straight, rather than a kinked, string the structure disappeared.

The total transverse mass of a set of particles in a rapidity bin, whether hadrons or partons, was also studied. The differential moments, the transverse mass moments for hadrons and the transverse mass moments for partons all showed the same structure, confirming that the source of the effect lay at the parton level. Finally, it was demon-

strated that the main features of the structure seen in the moments, and hence in the global moments, can be traced back to the first order matrix element level, coupled with kinematic bounds and the use of thrust to determine the event axis.

8 Acknowledgements

We thank W. Ochs for several useful discussions. We also thank the SL division for the excellent performance of the machine. We also wish to acknowledge the contribution made to ALEPH by the technical staff of CERN and the home institutes. Those of us not from member states thank CERN for its hospitality.

References

[1] A. Bialas and R. Peschanski Nucl. Phys. B273 (1986) 703, also Phys. Lett. B207 (1988) 59

[2] M. Bengtsson and T. Sjöstrand, Phys. Lett. B 185 (1987) 435

[3] W. Ochs Phys. Lett. B247 (1990) 101, Z. Phys. C50 (1991) 339, and private communication.

[4] T. Sjöstrand, QCD and Jets at LEP CERN-TH 5902/90

[5] G. Gustafson and C. Sjogren, LUTP 90-11

[6] G. Gustafson, LUTP 90-17

[7] M.Z.Akrawy et al.,(OPAL Collaboration), CERN-PPE/91-37

[8] P. Abreu et al.,(DELPHI Collaboration), Phys. Lett. B247 (1990) 137; A De Angelis, Mod. Phys. Lett. A5 (1990) 2395

[9] D. Decamp et al.,(ALEPH Collaboration), Phys. Lett. B234 (1990) 209

[10] D. Decamp et al.,(ALEPH Collaboration), Properties of hadronic Z decays and test of QCD generators, to be published.

[11] H.J. Behrend et al.,(CELLO Collaboration), Phys. Lett. B256 (1991) 97

[12] W. Braunschweig et al.,(TASSO Collaboration), Phys. Lett. B231 (1989) 548

Figure 1: Comparison of ALEPH data and GALEPH Monte Carlo for (a) standard and (b) normalized factorial moments in rapidity.

Figure 2: Normalized rapidity moments are compared with a simple two -parameter model.

Figure 3: Rapidity Distributions for: (a) ALEPH data; (b) GALEPH Monte Carlo; (c) generator level Monte Carlo; (d) generator level with cut on $p_t > 200 MeV/c$. The distributions are for charged tracks only and are normalized by the total number of entries and the rapidity interval.

Figure 4: Comparison of ALEPH data and GALEPH Monte Carlo for the third differential moment f_3. The solid line indicates the value of the corresponding global moment $F_3'(16)$ over the range $-2 < y < 2$.

Figure 5: ALEPH data showing the evolution of the third differential moment with number of rapidity divisions for a total of 8, 16 and 32 divisions in rapidity. The horizontal lines correspond to the values of the global moments $F_3'(M)$, $M = 4$, 8 and 16 respectivly.

Figure 6: Dependence of the differential moment on the choice of rapidity calculated with respect to the thrust or sphericity axis. The central dip is lost when the sphericity axis is used.

Figure 7: GALEPH Monte Carlo, and generator level Monte Carlo with and without a cut on transverse momentum of 200 MeV/c for the differential moment f_3. Working at generator level without the cut reduces the magnitude of the moments in the central region (partly by altering the normalisation) but does not affect the form of the y dependence.

Figure 8: Monte Carlo differential moment f_3 at generator level (a) with gluons switched off and default string fragmentation parameters, (b) with and without gluons for similar charged multiplicity $\langle N_{ch} \rangle$. The thrust axis was determined from the charged hadrons for both. The peaks near $|y| = 2.6$, clear in (a) but only just visible in

(b), are the result of the high multiplicity associated with b quark decay.

Figure 9: Transverse mass moment $\langle M_t^3 \rangle$, for data and Monte Carlo at the hadron level as a function of $|y|$.

Figure 10: Monte Carlo transverse mass moment at the generator level for (a) charged hadrons and (b) partons with and without gluons, showing the striking similarity in the behaviour of the moments at the two levels. The thrust axis was determined from the charged hadrons for both. The sudden changes just below $|y| = 3$ are associated with b quark events which have a maximum rapidity near this value.

Comparison of Data and Monte Carlo for Standard and Normalized 1-D Factorial Moments

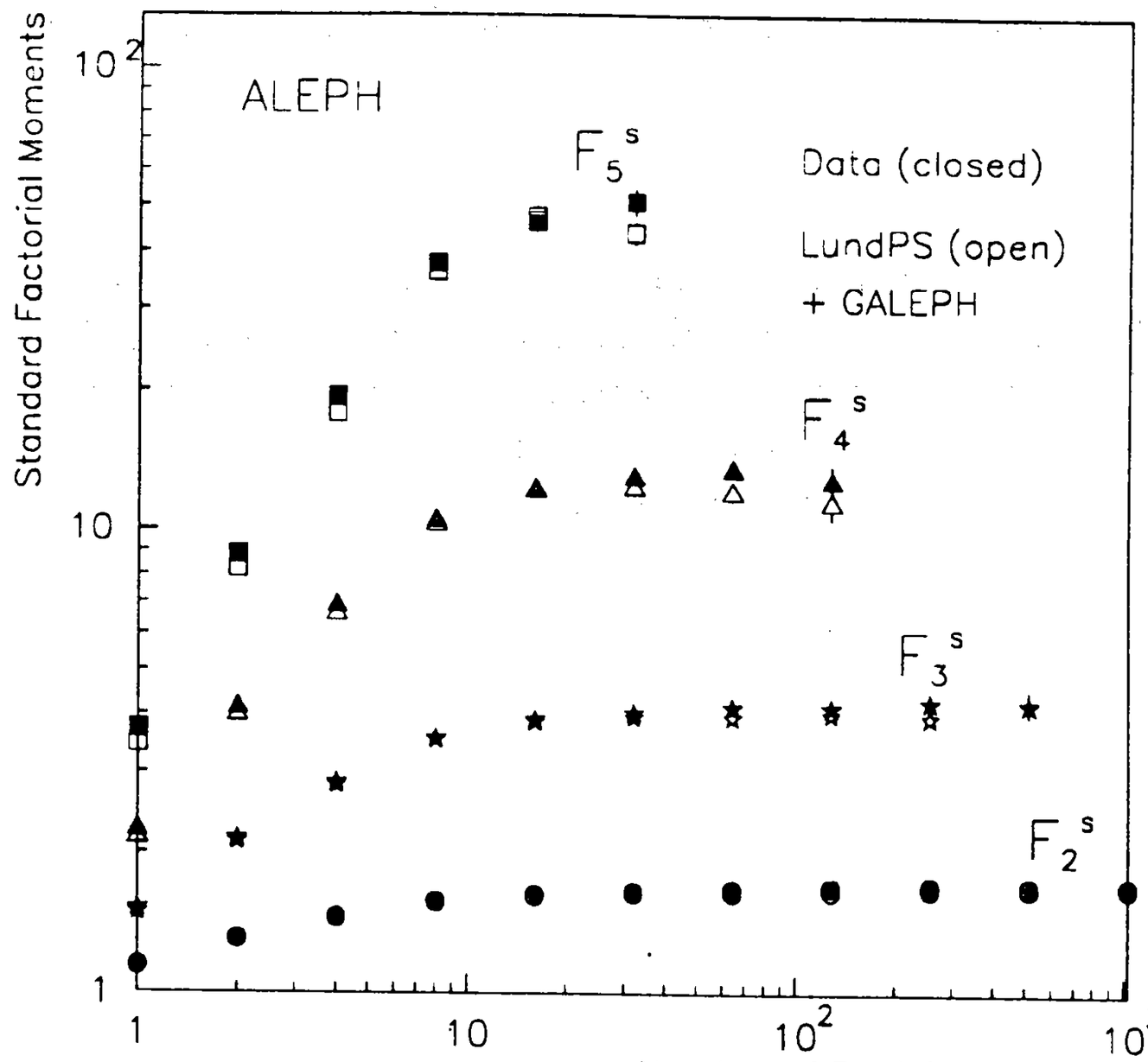

Figure 1a

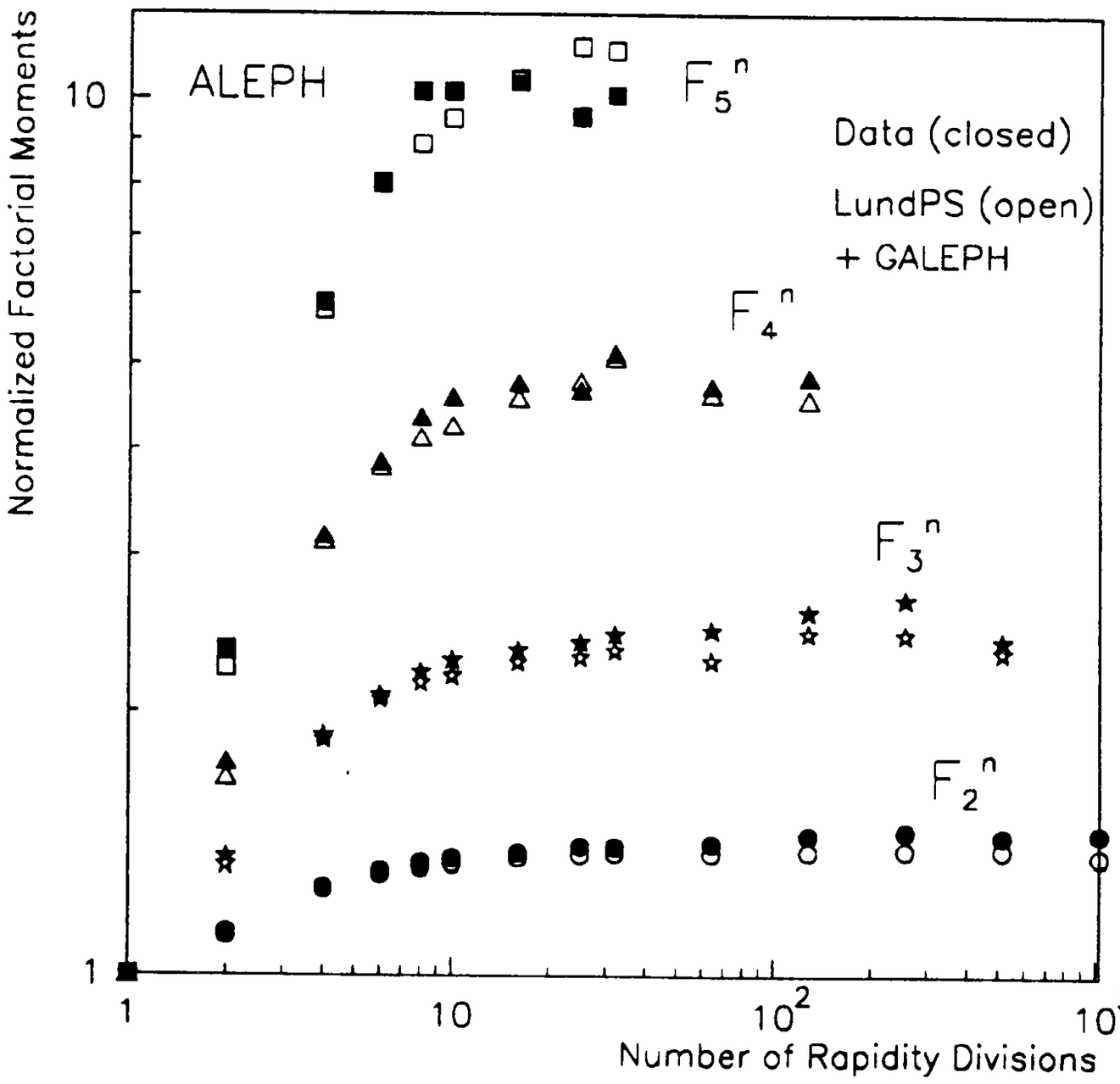

Figure 1b

1-D Normalized Moments and the Simple Model Data

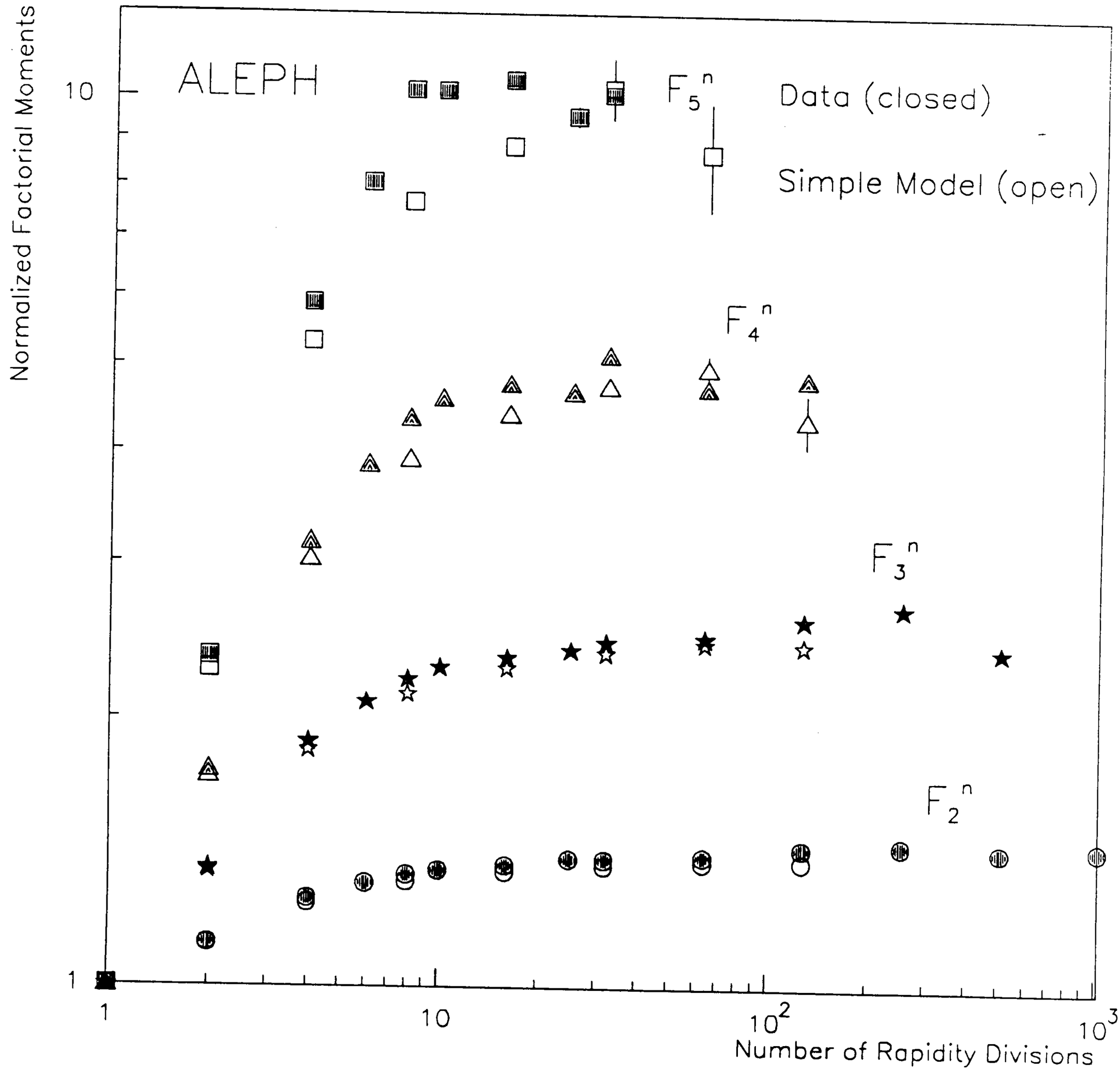

Figure 2

Normalized Rapidity Distributions

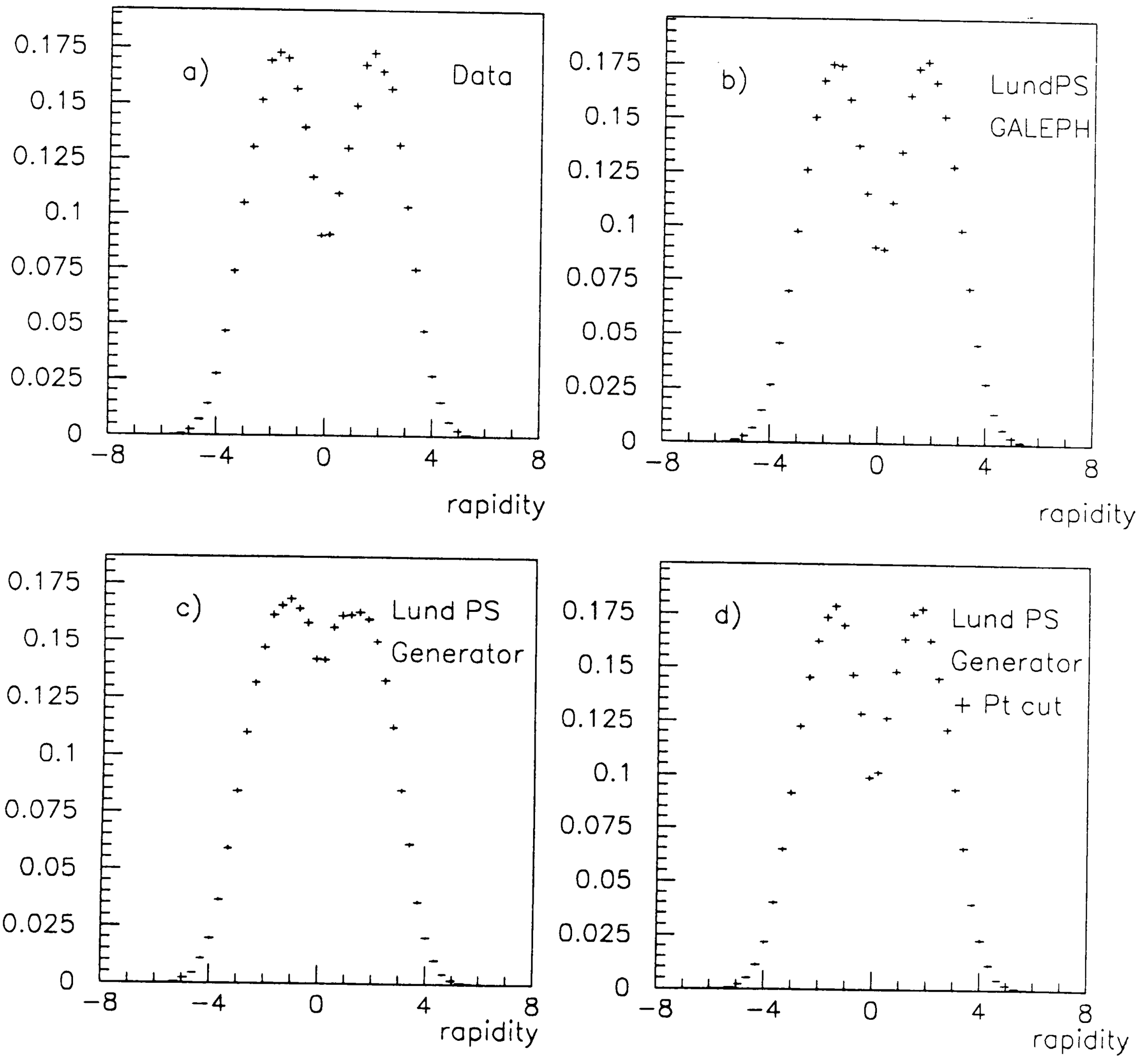

Figure 3

Comparison of Data and Monte Carlo for the Third Differential Moment

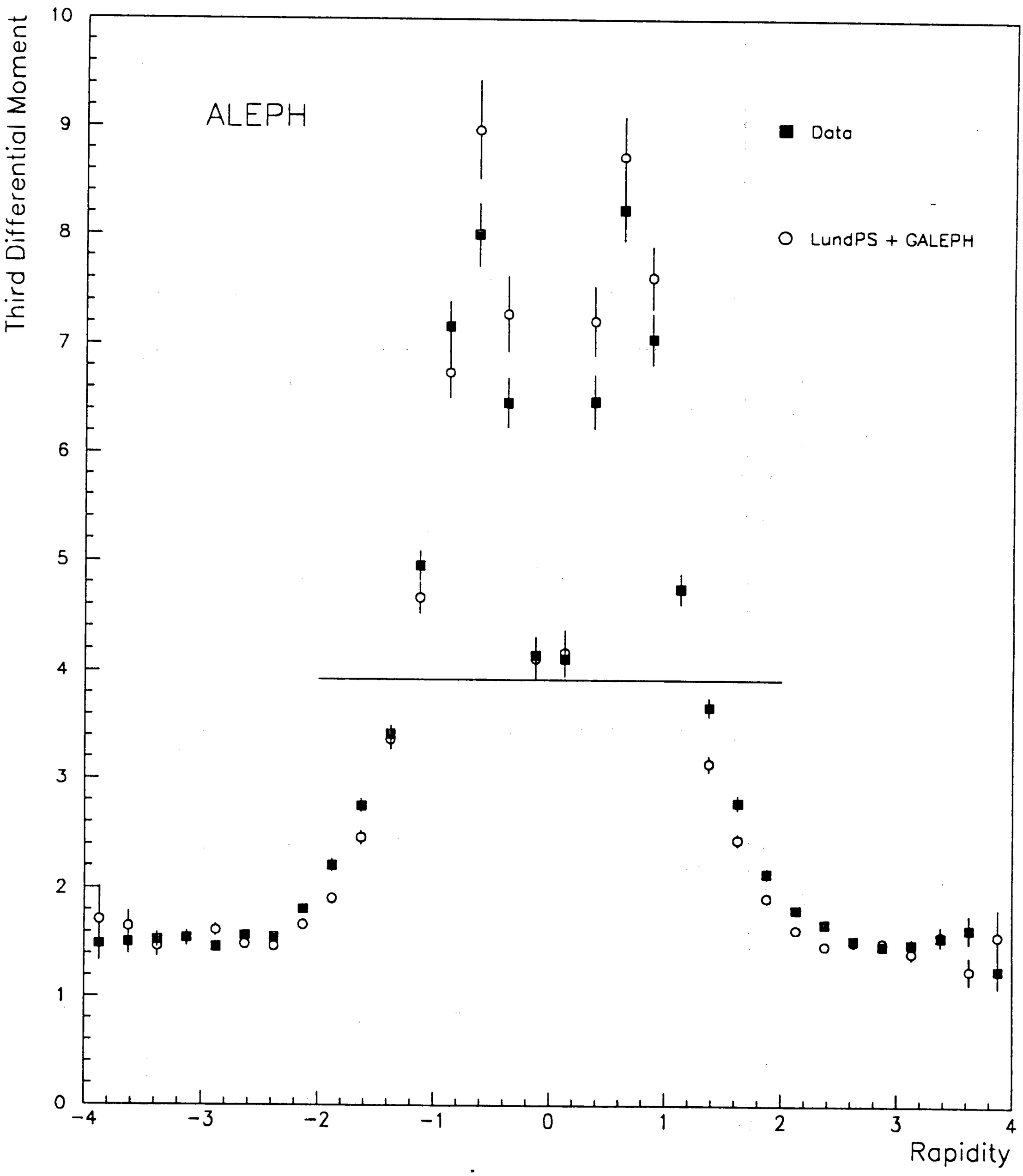

Figure 4

Variation in the Third Differential Moments with Number of Rapidity Divisions

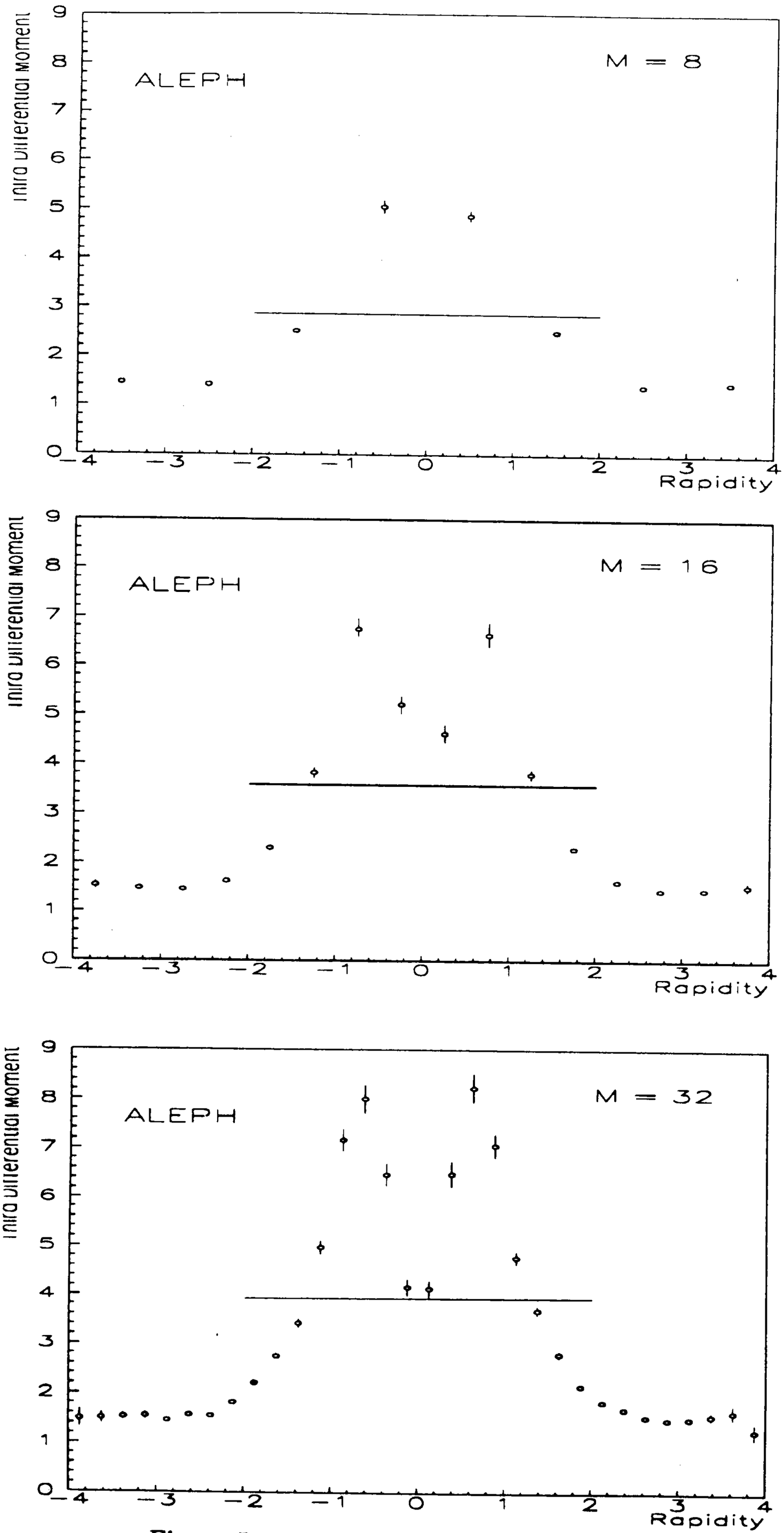

Figure 5

Comparison of Differential Moments with gluons on and gluons off

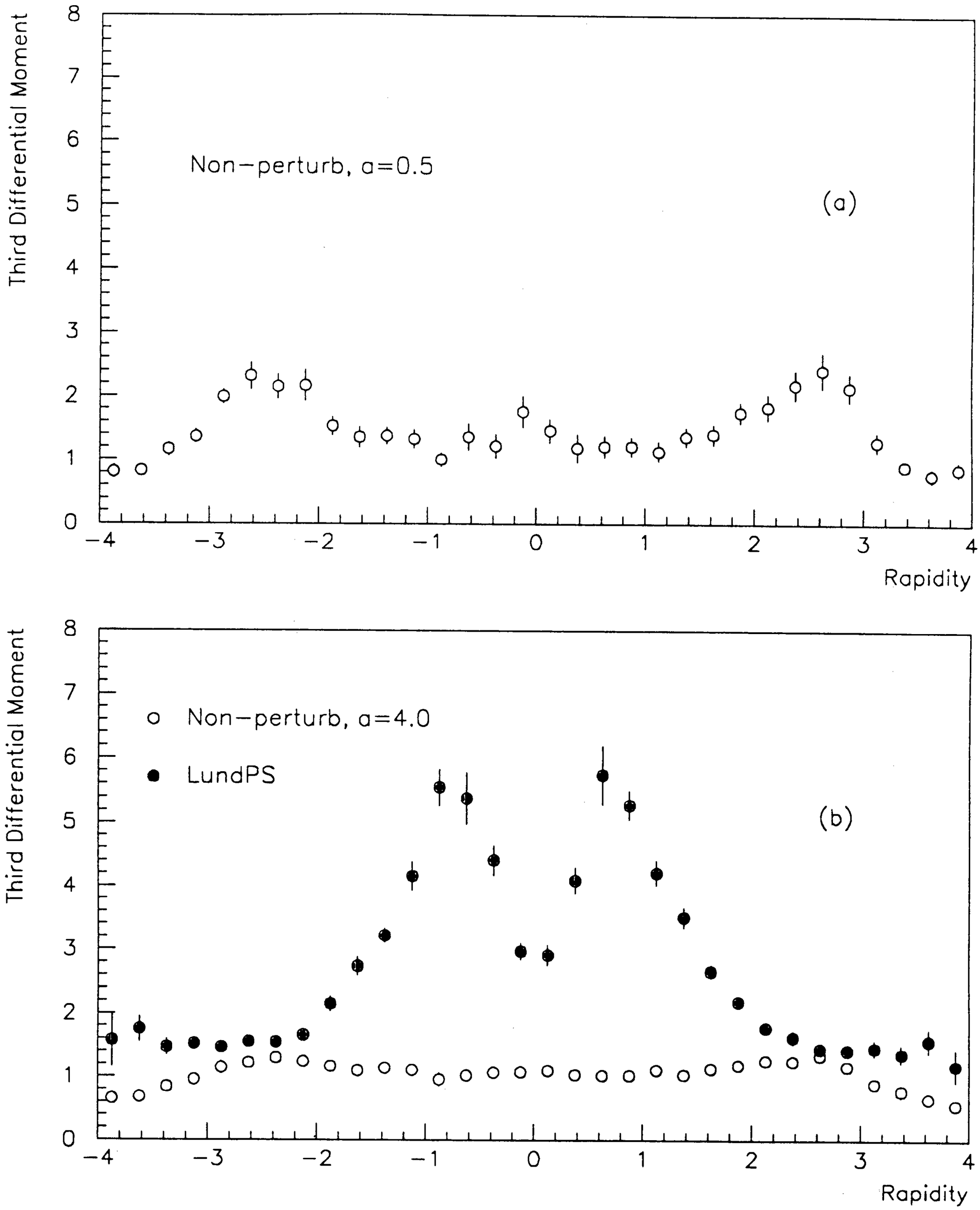

Figure 8

Reconstructed Monte Carlo, and Generator Level With and Without Transverse Momentum Cut of 200 MeV/c for Differential Moment

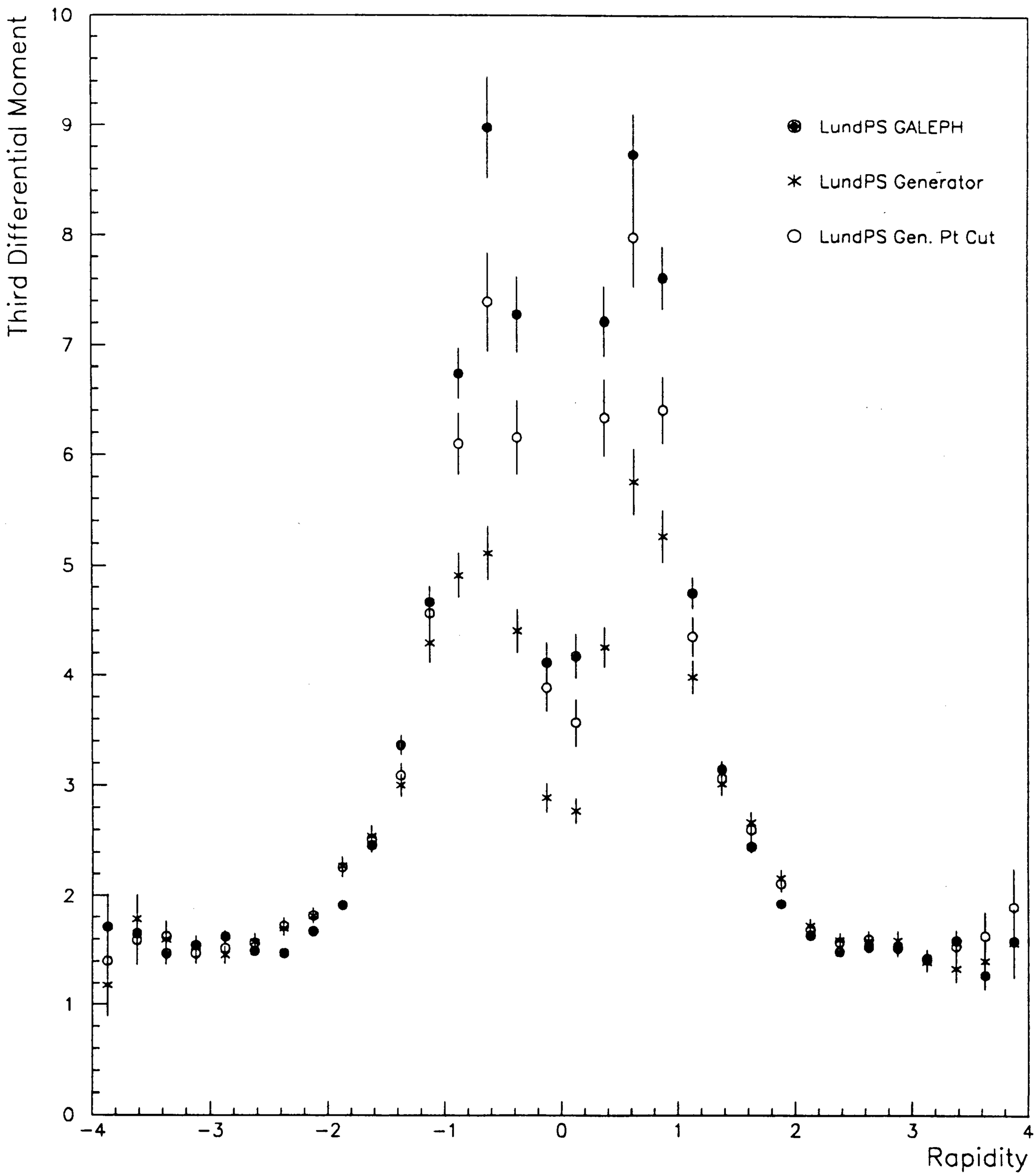

Figure 7

Transverse Mass Moments for Monte Carlo at generator level for hadrons and partons with and without higher order effects

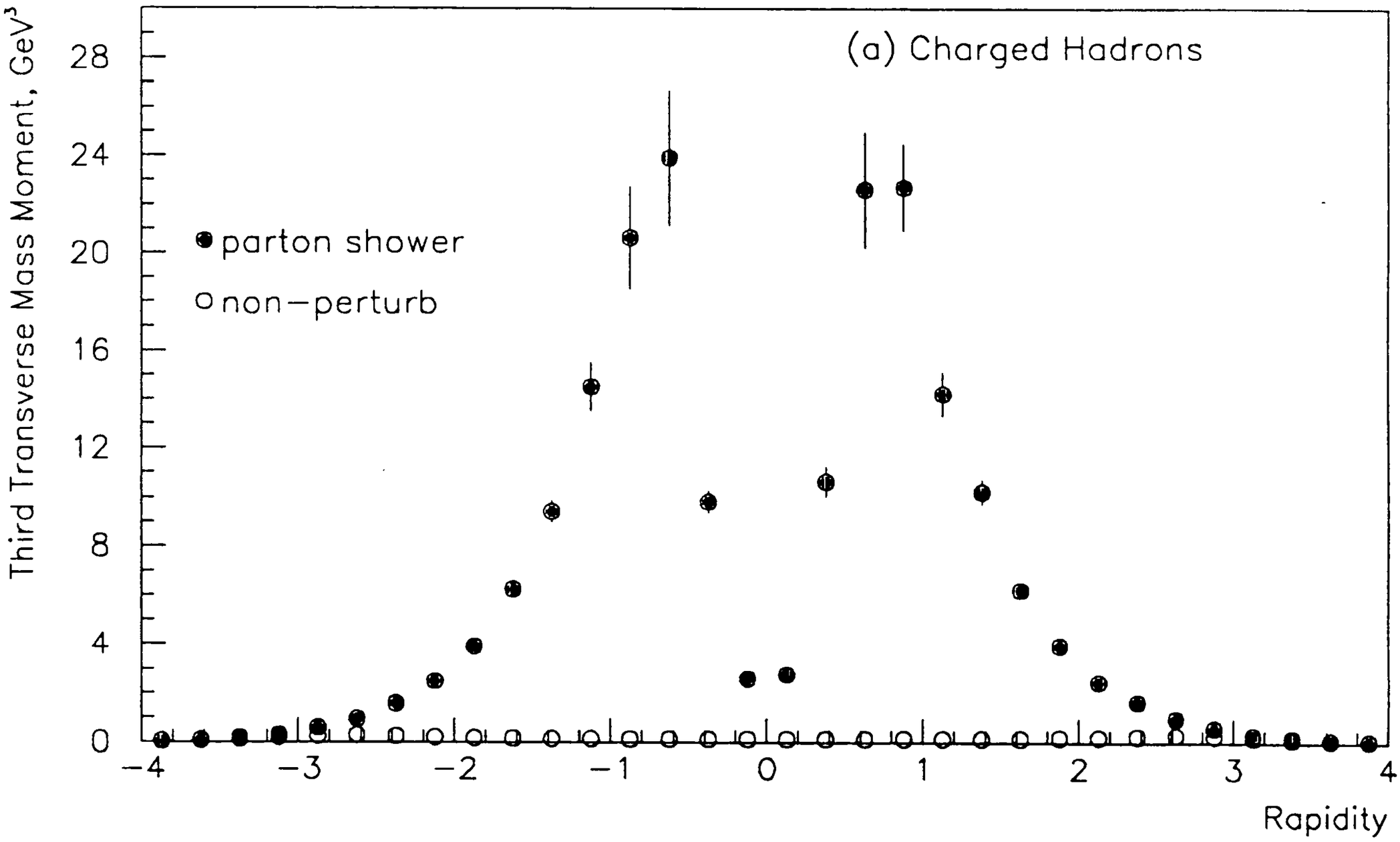

Figure 10

Imprimé au CERN. Prix: 0.90 Fr.

Transverse Mass Moments for Data at Hadron Level

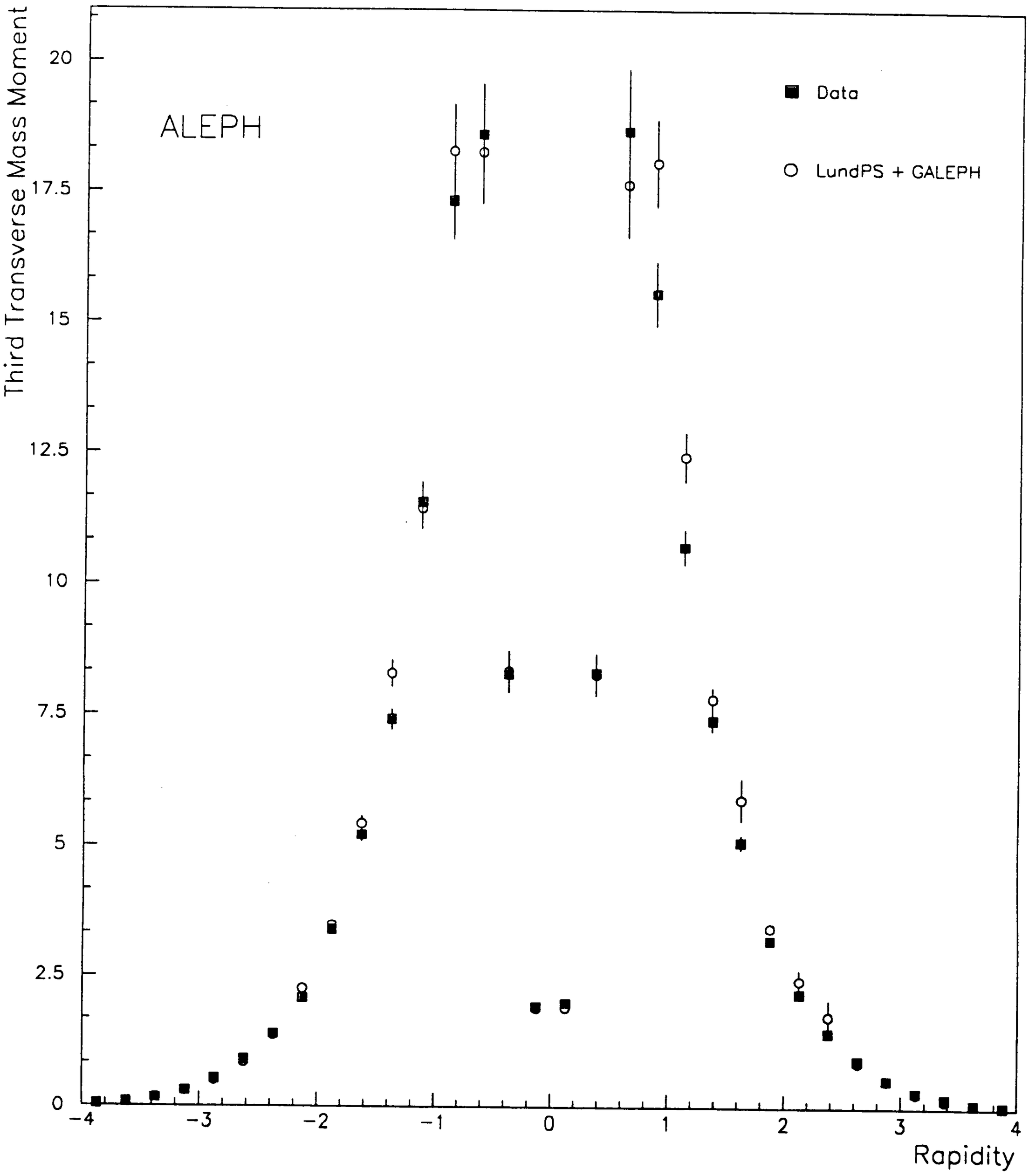

Figure 9